

Revisiting Limestone Quality for Soil Liming Purpose

Edson Campanhola Bortoluzzi ^{1,*}, Andressa Garibotti ², Tales Tiecher ³, Danilo Rheinheimer dos Santos ⁴, Diovane Freire Moterle ⁵ and Jackson E. Fiorin ⁶

¹ Laboratory of Land Use and Natural Resources, University of Passo Fundo, Campus I, BR 285, km 292, Passo Fundo 99052-900, RS, Brazil

² Faculty of Agronomy, University of Passo Fundo, Campus I, BR 285, km 292, Passo Fundo 99052-900, RS, Brazil

³ Interdisciplinary Research Group on Environmental Biogeochemistry, Department of Soil Science, Faculty of Agronomy, Federal University of Rio Grande do Sul, 7712 Bento Gonçalves Avenue, Porto Alegre 91549-000, RS, Brazil

⁴ Department of Soil Science, Federal University of Santa Maria, Roraima Avenue, 1000, Santa Maria 97105-900, RS, Brazil

⁵ Federal Institute of Education, Science and Technology of Rio Grande do Sul, Osvaldo Aranha, 540, Bento Gonçalves 995700-000, RS, Brazil

⁶ Cooperativa Central Gaúcha Ltda. CCGL., Cruz Alta 98005-970, RS, Brazil

* Correspondence: edsonb@upf.br; Tel.: +55-54-3316-8151

Abstract: The quality of lime is generally estimated by traditional methodologies, which consist of coarse granulometry and chemical reactivity determinations. Performing a detailed chemical/mineralogical and fine granulometric characterization is the objective of this study. Fifteen lime samples, from an original 52 commercial samples, were analyzed by their granulometric profile (GP) and chemical-mineralogical compositions to discuss limestone quality inside the tree group of traditional efficiency neutralizing power (ENP) and Mg contents. The lime reactivity was estimated using laser diffraction under water and acid solution (1 mol L⁻¹ HCl). The grain-size distribution ranged from 0.563 to 1124 µm and the GP was associated with the chemical and mineralogical compositions. Samples with high ENP (>99%) presented differences in GP regarding Mg contents. Lime with low ENP presents the most varied mineral assemblage, while calcite and dolomite were the predominant minerals in high-ENP samples. Samples containing high Mg were the most sensitive to the acid solution, suggesting great reactivity. This work contributes to a better understanding of limestone quality than routine analyses performed so far. Additionally, the use of the laser diffraction method promotes a rapid lime reactivity test for liming purposes.

Keywords: mineral dissolution; particle-size distribution; milling process

Citation: Bortoluzzi, E.C.; Garibotti, A.; Tiecher, T.; dos Santos, D.R.; Moterle, D.F.; Fiorin, J.E. Revisiting Limestone Quality for Soil Liming Purpose. *Minerals* **2022**, *12*, 1522. <https://doi.org/10.3390/min12121522>

Academic Editor: Nikolaos Kantiranis

Received: 25 October 2022

Accepted: 22 November 2022

Published: 28 November 2022

Publisher's Note: MDPI stays neutral with regard to jurisdictional claims in published maps and institutional affiliations.



Copyright: © 2022 by the authors. Licensee MDPI, Basel, Switzerland. This article is an open access article distributed under the terms and conditions of the Creative Commons Attribution (CC BY) license (<https://creativecommons.org/licenses/by/4.0/>).

1. Introduction

Liming is an agricultural practice that uses commonly, but not only, milling limestone in acid soil to increase soil pH, eliminate Al³⁺ toxic to plants, and supply Ca+Mg [1–3]. Due to lime application, the root system grows throughout a larger soil volume, leading to increased crop yield [2,4]. Liming is a complex and integrating practice, and its success depends on several factors related to the soil, the plant, and the quality of the liming product (i.e., stone mineralogy, chemical and milling process) [1–3]. Furthermore, changing the soil pH alters several other soil properties, such as the cation exchange capacity, base saturation, cationic micronutrient immobilization, soil particle aggregation, biological nitrogen fixation, and soil-water interaction [2,5–9].

Briefly, liming success depends only on chemical efficiency, which is the capability to produce OH⁻ and neutralize H⁺ from soil [10]. All remaining physicochemical soil changes are consequences of the decrease in proton activity in soil solution [3,6]. Currently in the literature, liming products' ability is associated with the chemical reactivity and

granulometric profile of limestone powders [4,8]. An efficacy index can be calculated as a common liming product quality indicator (i.e., equivalent neutralizing power—ENP). The ENP integrates the reactivity efficiency and neutralizing power [4]. In this sense, the liming product efficiency depends on its H⁺-neutralizing power and particle-size distribution after the milling process. However, traditional methods for estimating liming product efficiency were developed a half century ago for conventional soil management systems (i.e., where the soil disturbance reaches 20 to 30 cm depth).

Concerning the method of liming product application, it is well known that limestone incorporation up to 0.20 m depth allows better root system development for exploring great soil volume [10,11]. However, liming efficiency in in-depth H-neutralizing when lime is applied on the soil surface, takes time to react and reach deeper soil layers [1,3,12–14]. This occurs because lime migration in the acidic soil profile is also strongly dependent on the soil's physical properties, mainly linked to the water infiltration capacity [3]. These factors explain why there are contrasting results in the literature regarding the liming efficiency depth when lime is broadcasted on the topsoil [1,2,13]. Another scientific point concerns the proportion of Ca and Mg in the lime composition. Several studies have demonstrated that adequate crop yield is correlated with lime rate rather than the proportion of Ca:Mg present in lime [15,16].

The current challenge regarding liming is the application in a no-till system, where there is no soil disturbance and limestone powder is only broadcast on the soil surface. In these conditions, we expect that the neutralization of soil acidity in-depth after topsoil liming application will become more dependent on the mineralogical composition and grain-size distribution profile after the milling process. Thus, a detailed chemical/mineralogical characterization of lime powders must be considered in order to estimate the lime efficiency of lime powders.

In the literature, the alkaline/calcareous rock characterization has been of geological interest [17]. For instance, Olego et al., 2021 [7] stated that liming material is a crucial step for choosing an adequate limestone product for the liming purpose of acid soils. However, few studies have been devoted to exploring limestone quality, including methodology improvement, mineral characterization, and the relationship between chemical parameters and particle-size distribution for agricultural purposes. In addition, the literature is relatively vast with regard to the liming effect on soil properties, including biological, chemical, and physical ones [6,7].

The objective of this work was to evaluate the chemical and mineral composition of lime, as well as to associate them with the grain-size distribution of commercial liming products for acidity correction (limestones/oxides/hydroxides) commonly used in acid soil under the no-till system from Brazilian agriculture. We will discuss whether liming products with different calcium (Ca) and magnesium (Mg) compositions and grain-size distribution present similar reactivities estimated by the ENP. Our results may aid in defining a new methodological basis for liming product choice and more efficient liming practice, as suggested in the literature [7].

2. Materials and Methods

2.1. Strategy of Study

This study took powder aliquots of 52 commercial liming products from many parts from Southern Brazil. The sample collection was sent to the commercial laboratory at the University of Passo Fundo for an exploratory study promoted by CCGL/RTC and FE-COAGRO/RS. The liming products were analyzed based on the chemical composition and ENP parameter [18].

For the ENP estimation, we used limestones/correctives samples after drying at 105° C.

$$\text{ENP} = (\text{RE} * \text{NP})/100 \quad (1)$$

where RE is the reactivity efficiency and NP is the neutralizing power.

For this, two aliquots were taken: one aliquot of 1 g was taken for the chemical neutralizing power measurement. The sample was placed inside a 250 mL flask (Erlenmeyer type) and 50 mL of 0.5 mol L⁻¹ HCl solution was added. Afterward, the flasks were boiled for 5 min. The solution was transferred to a 100 mL volumetric flask and the volume was completed with distilled water. Using a volumetric pipette, 50 mL of the supernatant solution was transferred to an Erlenmeyer flask of 100 mL. Next, 3 drops of a phenolphthalein solution, as an indicator, was added and the titration was made using 0.25 NaOH mol L⁻¹ solution to neutralize the acid excess. The NP was calculated as follows, relative to ultra-pure CaCO₃:

$$NP = 10 * [(20 * M1) - (Vb * M2) * G] \quad (2)$$

where M1 = concentration of HCl solution (mol L⁻¹); Vb = volume (mL) of the NaOH used for the titration; M2 = concentration of NaOH solution (mol L⁻¹); and G = initial mass of sample (g).

Another aliquot was used to estimate chemical reactivity based on the particle-size distribution. For this, 100 g of lime powder was placed in a sieve shaker device, which contained sieves with diameters of 2 mm (S1), 840 µm (S2), and 300 µm (S3). The reactivity was calculated as follows:

$$RE = 0.2 * (S1-S2) + 0.6 * (S2-S3) + S3 \quad (3)$$

where S1, S2, and S3 are the mass retained in each sieve.

Based on the ENP results, 15 samples were selected to represent three groups of ENP: (i) 70–80%, (ii) 80–99%, and (iii) >99%. Furthermore, for each group, the samples were separated into sub-groups that had low- and high-magnesium content. Details of this strategy are shown in Table 1.

Table 1. Groups of limestones/correctives product samples based on the efficiency neutralizing power and MgO and CaO contents.

Samples	ENP/MgO Contents		2 mm Mesh	Retained 0.84 mm Mesh	0.3 mm Mesh	NP (%)	ENP (%)	MgO (%)	CaO (%)	Ca/Mg Ratio
1	70–80	high Mg	0	14.4	28.7	102.03	78.56	10.12	31.43	3.7
2			0	19.1	30.6	104.23	75.55	10.16	28.16	3.3
3			0	19.4	35.0	103.19	72.73	10.12	28.65	3.4
4	80–99	high Mg	0	6.5	13.0	108.88	97.56	10.09	29.28	3.4
5			0	12.0	22.5	111.44	90.71	10.06	30.08	3.5
6			0	7.0	15.3	110.51	97.56	10.45	29.99	3.4
7		low Mg	0	7.2	24.5	104.24	88.02	5.51	43.2	9.3
8			0	9.2	25.6	100.29	82.64	6.55	37.92	6.9
9			0	8.6	20.4	104.35	88.66	7.01	45.16	7.6
10	>99	high Mg	0	0	0	99.47	99.47	10.32	30.53	3.5
11			0	0	0	159.89	159.89	10.59	30.62	3.4
12			0	0	0	155.94	155.94	10.08	38.64	4.5
13		low Mg	0	0	0	105.37	105.37	0.61	43.1	83.7
14			0	0	0	99.13	99.13	0.56	45.92	97.1
15			0	0	0	107.72	107.72	0.51	56.72	131.7
min	n = 52						69.2	0.5	23.0	
mean	n = 52						88.2	5.6	31.6	
max	n = 52						159.9	10.6	56.7	

Efficiency neutralizing power (ENP).

2.2. Limestone Powder Characterization

The samples were separated into three size-particle fractions (i.e., total, >0.30 mm, and <0.30 mm fractions), and they were characterized by their chemical and mineralogical compositions.

Total chemical composition was performed using an S2 Ranger energy dispersive X-ray fluorescence device (EDXRF) (Bruker®, Billerica, MA, USA). The samples were pre-treated as follows: the limestone samples were dried at 45 °C for 48 h, and 7.0 g of powder was mixed with 3 g of H₃BO₃ and pressed at 25 tons per cm² using a Fluxana Press device (Fluxana®, Bedburg-Hau, Germany) to form pellets. The pellets were placed in the S2 device and the operational configuration measurements were made as follows: measurements in triplicates; atmosphere using helium gas. The chemical results are given in the oxide form, expressed in mg kg⁻¹.

2.3. Mineral Composition

The mineralogy was performed using an X-ray diffraction (XRD) device, model D2 Phaser (Bruker®). The configuration of operation was at 30 w and 15 mA. The powder in three fractions (whole fraction, <0.3 mm, and >0.3 mm fractions) were recorded in XRD patterns between degrees 5–65° 2theta at the step of 0.02°.

The mineralogical composition was estimated according to Brindley and Brown [19], comparing the XRD pattern peaks with the reference mineral's peaks. We also used DiffracEVA software (Bruker®) to find the minerals in the Crystallography Open Database (COD) mineral base.

2.4. Particle Size Distribution Using Laser Diffraction

The particle-size distribution (PSD) was carried out using a laser diffraction device (LD) model Bettersizer S2-WD®, operating in a liquid media recording grain-size ranging from 0.02 µm to 2000 µm. This device uses the Mie theory as the optical model; details of the methodology may be found in the literature [5]. The powder limestone samples (whole fraction < 300 µm) were recorded in triplicates. One gram of each sample was pre-prepared as follows: (i) the samples were suspended in a Becker flask in 50 mL of distilled water, under agitation, and then the suspension was introduced in the LD chamber, and after 1 min under agitation, the PSD was estimated and recorded; (ii) in the same Becker flask, 5 mL of 1 mol L⁻¹ HCl solution was added to the sample, and a new LD new measurement was performed after 1 min; (iii) the measurements were repeated after 5 min. In this way, the same samples produced three size profiles (i.e., with only water, after adding HCl, and recording after one and five minutes). The HCl concentration chosen was in accordance with reactivity analysis of liming products and aims to have a H⁺ surplus favoring the acid/base reaction, engendering mineral dissolution [8,10,18]. We expect the granulometric profile of the liming products to change as a consequence.

2.5. Statistical Analysis

A descriptive analysis was performed on all samples (52 samples). Principal component analysis (PCA) was carried out on the data using 15 samples, considering a $p < 0.1$. The principal component analysis explains the correlation degree among the variables. The axes PC1 and PC2 explain, in an orthogonal manner, the strongest magnitudes of data variability by percentage [20].

3. Results

3.1. Descriptive Analysis of Chemical Composition and Reactivity

Overall, the whole set of 56 liming product samples presented ENP values ranging from 69.2 to 159.9% (mean of 88.2%—Table 1). The calcium (CaO) content ranged from 23.0 to 56.7% (mean of 31.6%), while magnesium (MgO) content ranged from 0.50 to 10.6% (mean of 5.6%).

Regarding the 15 liming products samples (Table 1) only: they were selected for detailed mineralogical, chemical, and granulometric analysis. We found the mass ratio of Ca to Mg for these samples ranged from 3.3 to 131.7 (Table 1). For the group I (lower ENP: ~70–80%), only samples with high Mg content were found. The samples from group II, presented two sub-groups: low Mg content (~6.0% of MgO) and high Mg content (~10.0% of MgO). The mass ration of Ca to Mg was approximately 3:1 for the subgroup with high Mg and 7:1 for the subgroup with low Mg content. In group III, the mass ratio of Ca to Mg was approximately 3:1 for the subgroup with high Mg and 88:1 for the subgroup with low Mg content (Table 1).

All subgroups with high Mg content presented a similar proportion between Ca:Mg (around 3:1), but placed in different ENP groups (Table 1). This suggests a similar chemical composition but different cation-bearing mineralogy.

The samples with ENP from group I (ENP < 80%) presented a varied chemical composition mainly composed of CaO and MgO, but presenting SiO₂, Al₂O₃, Fe₂O₃, K₂O, Cl, TiO₂, P₂O₅ e SrO in their composition (Figure 1). Lime with high ENP presented a simpler chemical composition, based only on CaO (low Mg content) or in combination with low Mg content (Figure 1).

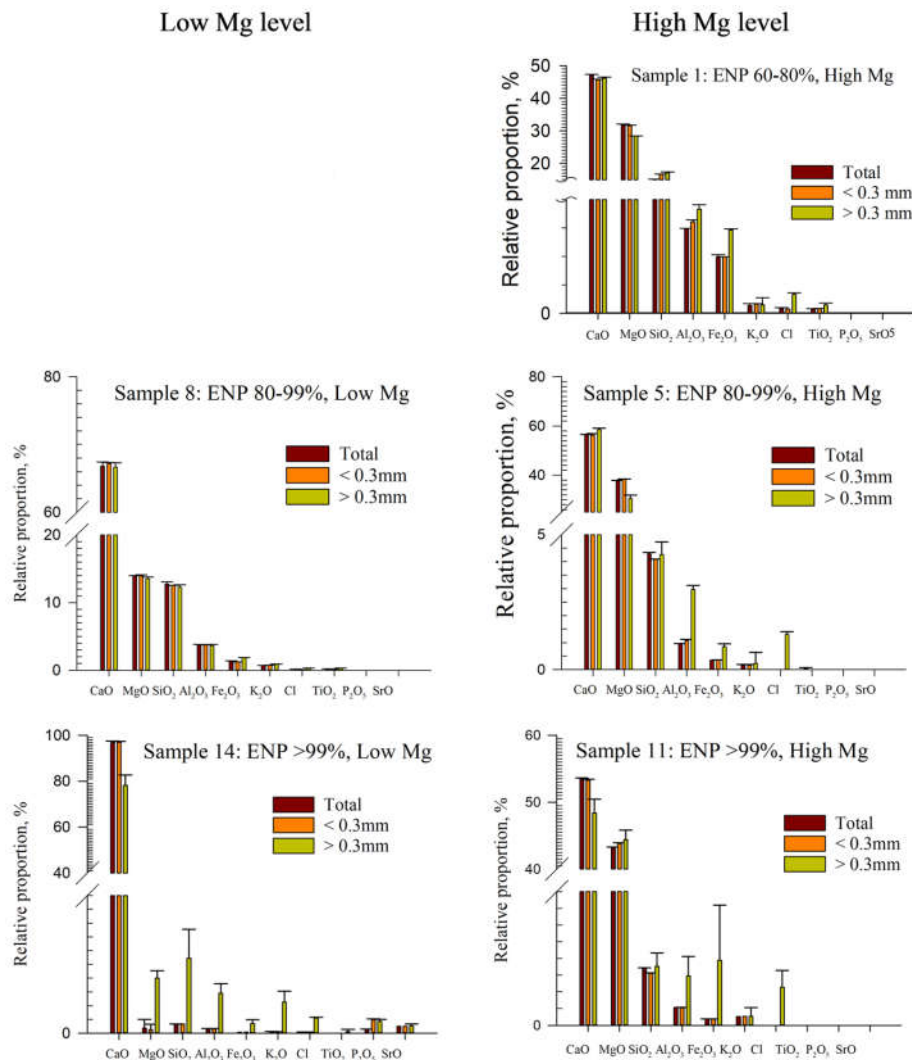


Figure 1. Chemical composition using X-ray fluorescence by dispersive energy from representative lime/corrective samples separated into three groups of efficiency neutralizing power—ENP and two Mg levels (low and high). The samples’ number correspond to the samples described in Table 1.

Lime with low ENP presented a higher proportion of SiO₂, Al₂O₃, and Fe₂O₃, indicating the presence of aluminosilicates minerals, as sample 01 (Figures 1 and 2; Table 2). Al contents (Al₂O₃) can reach values as high as 4% (Figure 1). These mineral compounds did not affect soil acidity and, therefore, are contaminants (Figure 1). The high MgO content was associated with low aluminosilicates minerals content.

Table 2. Mineral composition and quantification based on the X-ray diffraction (XRD) patterns from limestone/corrective powder samples.

Samples	Mineral	Ideal Chemical Formula	XRD Peaks (d = nm) Intensity(I/I ₀)	Relative Proportion %
(1), 2, 3	Ankerite	CaFe ₂ + 0.6Mg0.3Mn ₂ + 0.1(CO ₃) ₂	0.289(1), 0.181(0.06), 0.219(0.06)	44.1
	Dolomite	CaMg(CO ₃) ₂	0.288(1), 0.178(0.6), 0.219(0.5)	37.6
	Sillimanite	(Al ₂ O ₃)(SiO ₂)	0.342(1), 0.337(0.65), 0.22(0.6)	8.9
	Otavite	Cd(CO ₃)	0.295(1), 0.378(0.8), 0.246(0.35)	3.8
	Calcite	CaCO ₃	0.303(1), 0.209(0.18), 0.228(0.18)	1.3
	Mica		1.00	~
4, (5), 6	Dolomite	CaMg(CO ₃) ₂	0.288(1), 0.178(0.6), 0.219(0.5)	84.5
	Ankerite	CaFe ₂ + 0.6Mg0.3Mn ₂ + 0.1(CO ₃) ₂	0.289(1), 0.181(0.06), 0.219(0.06)	7.4
	Otavite	Cd(CO ₃)	0.295(1), 0.378(0.8), 0.246(0.35)	5.8
	Quartzo	SiO ₂		0.6
7, (8), 9	Calcite	CaCO ₃	0.303(1), 0.209(0.18), 0.228(0.18)	54.0
	Dolomite	CaMg(CO ₃) ₂	0.288(1), 0.178(0.6), 0.219(0.5)	36.1
	Quartzo	SiO ₂		8.7
	Otavite	Cd(CO ₃)	0.295(1), 0.378(0.8), 0.246(0.35)	1.2
	Mica		1.00	~
10, (11), 12	Calcite	CaCO ₃	0.303(1), 0.209(0.18), 0.228(0.18)	66.3
	Portlandite	Ca(OH) ₂	0.262(1), 0.49(0.74), 0.192(0.42)	14.3
	Periclase	MgO	0.210(1), 0.148(0.52), 0.122(0.12)	13.8
13, (14), 15	Calcite	CaCO ₃	0.303(1), 0.209(0.18), 0.228(0.18)	87.1
	Briartite	Cu ₂ Zn _{0.75} Fe _{2+0.25} GeS ₄	0.306(1), 0.187(0.5), 0.189(0.5)	1.2

Relative proportion among mineral assemblage was obtained in the Diffrac-EVA software. The numbers between parentheses correspond to the sample's number presented in Table 1.

As can be seen in sample 14 from group III (>99% ENP) with low MgO content (Figure 1), the overall concentration of MgO is very low, but in the particle-size fraction > 0.3 mm, the concentration of MgO is 5.6%. The highest MgO content among the lime samples was approximately 40% in sample 11 (Figure 1).

Regarding the particle-size fraction evaluated, for samples 14, 11 (ENP > 99), and 5 (ENP 80–99%) the > 0.3 mm fraction presented lower CaO content than the other fractions, indicating mineral selectivity by size. Furthermore, sample 5 presented in the > 0.3 mm fraction lower MgO content than the other fractions. The K₂O varied among the fraction for samples 11 and 14, presenting ~3% of K in the fraction > 0.3 mm.

3.2. Mineralogical Assemblage

Lime with low ENP (group I) was associated with a rich mineral assemblage, composed basically of ankerite, dolomite, and sillimanite minerals, while calcite mineral content was found in a proportion lower than 1.5% (Figure 2 and Table 2). Group II was very

similar in mineralogical assemblage to group I, but the dolomite proportion was bigger in the mineral assemblage. Lime with high MgO content was associated with dolomite mineral presence for samples 1 and 5 (groups I and II).

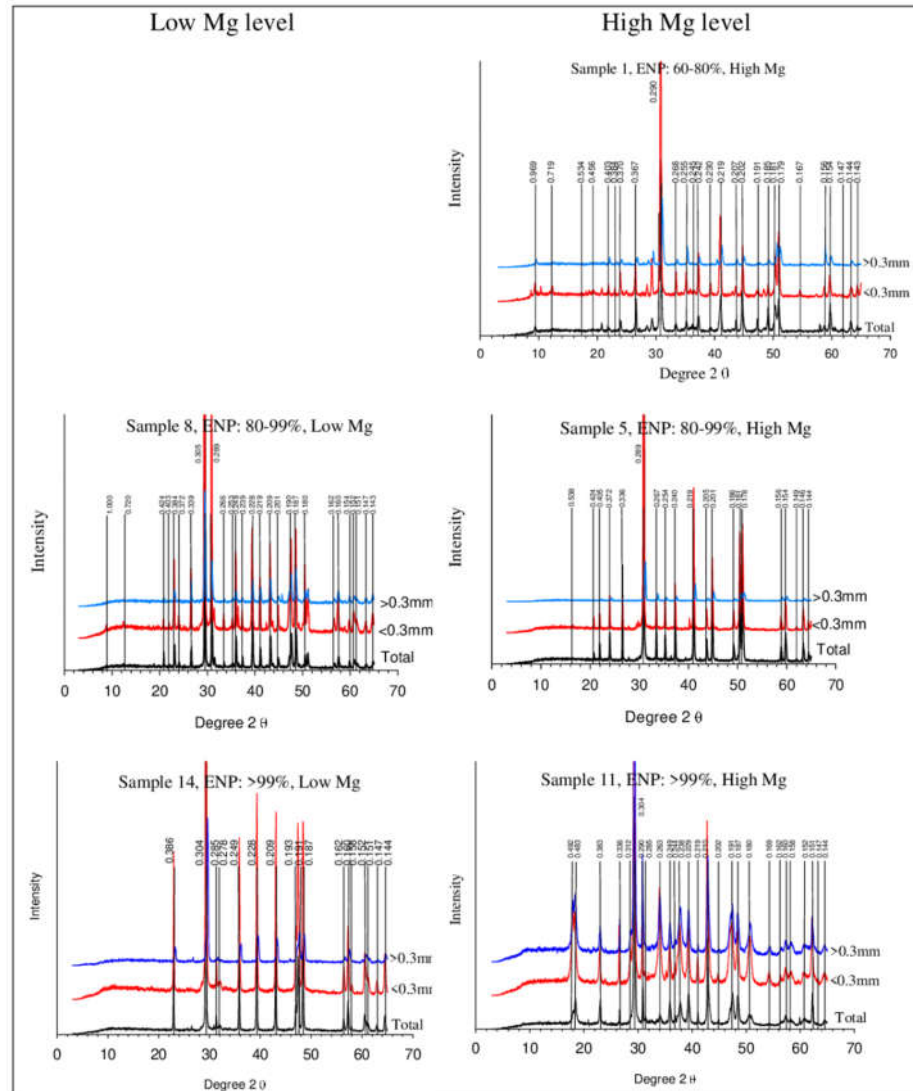


Figure 2. X-ray diffraction patterns from representative liming products (in three fractions) were separated into three groups of efficiency neutralizing power (ENP) and two Mg levels (low and high).

Lime with high ENP (group III) was associated with a simpler mineral assemblage, composed basically of calcite and portlandite minerals at more than 66% and 14%, respectively (Figure 2 and Table 2), while lime with high MgO was associated with the presence of periclase (samples 11).

3.3. Particle Size Profile

The grain-size distribution of the samples ranged between 0.563 to 1124 μm . The limestone with low ENP (70–80%) still had coarse particles (Table 1; Figure 3). The most notable peak was at 200–300 μm , followed by the particles around 20 μm (Figure 3).

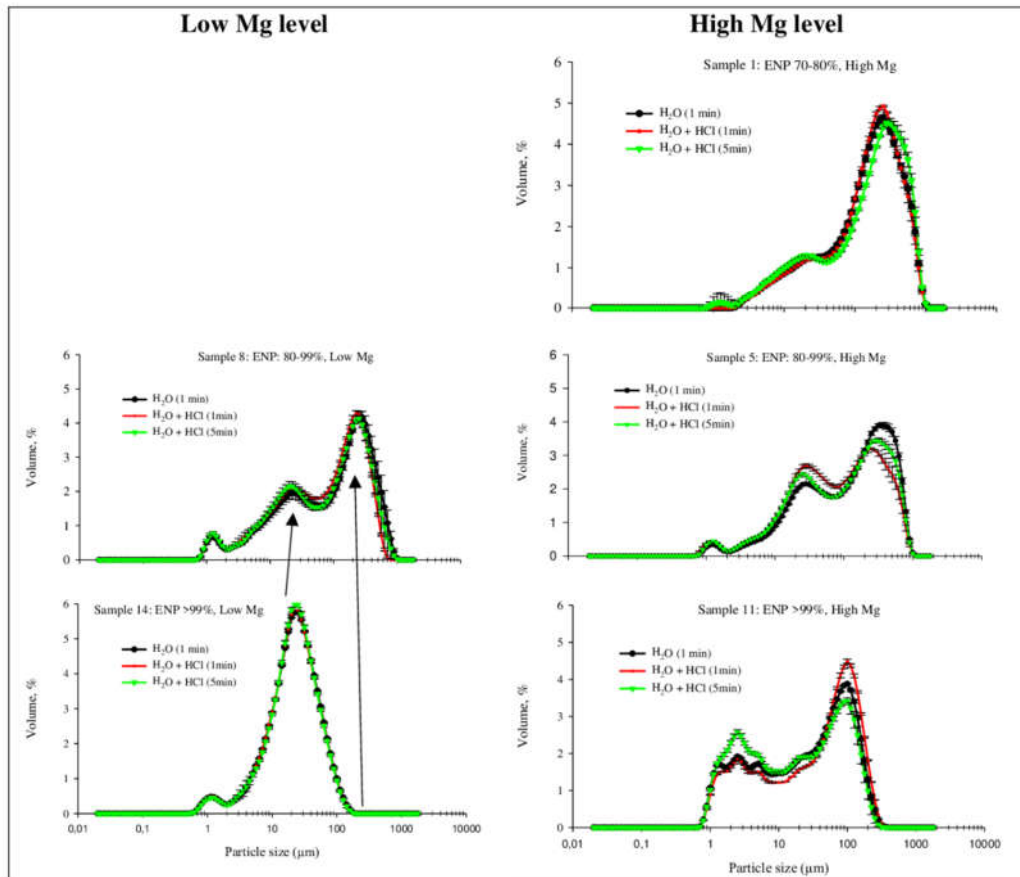


Figure 3. Diffraction laser granulometric profiles from representative lime/corrective samples were separated into three groups of efficiency neutralizing power (ENP) and two Mg levels (low and high).

Limestone samples with intermediate ENP (80–99%) presented a wideband composed of three peaks from 1–1000 μm , with larger particle volume at bigger particle size (200 to 300 μm), with an increase in particle size between 10 and 50 μm in all particles smaller than 100 μm , and with a huge volume of extremely fine particles (1 and 10 μm) in those with ENP > 99%.

Limestone samples with higher ENP values (>99%), regardless of the MgO content, had higher proportions of finer particles, concentrated at 1 and 20 μm peak positions (Figure 3). Peaks bigger than 100 μm are absent.

Concerning MgO content, limestones were very similar between low and high Mg content. However, the particle size distribution from the Mg-rich limestone at high ENP presented the largest volume of extremely fine particles (<10 μm).

Overall, the granulometric profile (GP) was slightly sensitive to the acid treatment in all the lime samples, except for sample 11 (high ENP and high MgO). For this sample, there was an enrichment of the proportion of particles at 2 μm diameters, in detriment to those at 100 μm . The sample in group III and the subgroup with low Mg were not sensitive to the acid solution exposure.

In general, lime acid exposure diminished the volume proportion of larger particles from lime, and there was no small-particle production, indicating that a dissolution process occurred.

As expected, there are strong associations between calcite and CaO content and dolomite with MgO content. This is indicated by the length of the vectors and their directions (Figure 4). However, the presence of calcite is the opposite of the dolomite presence, i.e.,

the vectors were in opposite directions. In this sense, three principal groups of limestone may be observed as chemical and mineralogical assemblage: (i) limestone with high calcite and CaO content, (ii) limestone with high dolomite and MgO content, and (iii) limestone presenting other minerals in its composition—such as periclase, portlandite, and ankerite—which had a strong association with RE and ENP (Figure 4). Ankerite occurrence can be associated with large particles in the lime GP because this mineral had Fe in its composition. Lime that presented sillimanite and quartz was associated with large particle size and low acid-neutralizing capacity.

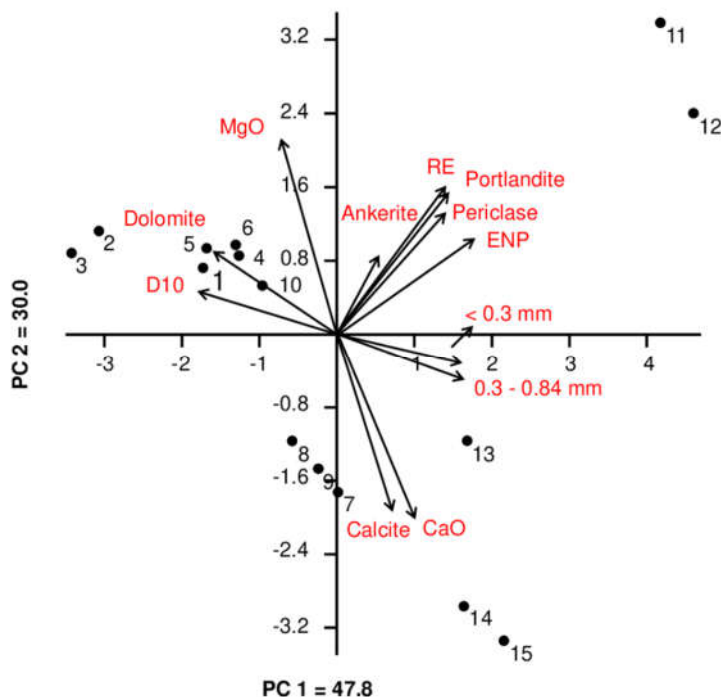


Figure 4. Principal component analyses considering liming product samples (number), mineralogy, and physical and chemical analyses of liming product samples. Data set used for ($n = 15$ samples). The principal components (i.e., axes PC1 and PC2) explain the magnitudes in the percentage of data variability. D10 is the % of particle size smaller than 10%. <0.30 and 0.3–0.84 mm corresponding to the size fractions. RE is the reactivity efficiency and ENP is efficiency neutralizing power.

4. Discussion

Overall, lime quality (ENP) is directly associated with the milling process, and it can be analyzed with a routine method in which liming product samples are classified based on their acidity-neutralizing capacity. In this study, we focused on the most reactive particle fractions from limestone; thus, it was possible to observe that the chemical and mineralogical components of lime are associated. In addition, a large proportion of fine particles present in our samples have a granulometry profile, containing microparticle size, but not nanoparticles, which characterizes high reactivity in the environment. Below, we discuss in detail these aspects:

Limestone has been used since the early days of agriculture because of the presence of carbonate anion [10,14]. This anion, in an aqueous medium, easily breaks up water molecules, generating two new anions (HCO_3^- and OH^-) capable of instantly reacting with protons. These anions are essential to adapting acidic soil to crops sensitive to the toxicity caused by Al^{3+} present in soil with $\text{pH} < 5.5$. In addition to carbonate, some limestone used in agriculture also have low amounts of oxides and hydroxides, which increase the neutralizing power of the acidity [4].

Naturally, the carbonates are counterbalanced by the calcium and magnesium cations [17]. They are nutrients to all living things, including and especially to plants, which transfer them up the food chain. Rarely, there can be impregnation of Ca and Mg carbonates with trace metal elements—especially Cd, Mn, and Fe—or even the occurrence of pure carbonates of these elements, as is the case with Otavite.

The world's reserves of Ca and Mg carbonates are either of sedimentary or metamorphic origin. Both are not pure rocks; nor do the rocks consist solely of carbonate ores. Thus, limestone for agricultural use will always have “contaminating” minerals to some degree. The limestone from the Brazilian cretaceous can be seen in detail in Gomes et al. [17]

Therefore, the use of large amounts of limestone (up to 30 Mg ha⁻¹), as is the case in soil occurring in tropical and subtropical regions, introduces chemical elements to the soil, whether they are essential or ecotoxic. Three examples can be explained based on our mineralogical analyses. First, the presence of aluminosilicate minerals that follow the weathering process (hydrolysis) may release Al³⁺ to the soil, becoming a potential toxic element source. Second, the limestone containing K (such as sample 11 with 3% K₂O) can represent an application in the soil of 30 kg of K₂O ha⁻¹ t⁻¹. However, K-bearing minerals, such as tectosilicate (feldspar), present low dissolution rates, and by consequence, low K bioavailability. And third, although it has lower solubility (1.0×10^{-12} mol L⁻¹) compared to the traditional carbonates found in limestone (3.31×10^{-9} and 9.33×10^{-9} mol L⁻¹ for calcite and magnesite), the high amount of CdCO₃ (5.8% Otavite) present in sample 4 can release Cd²⁺ to the soil solution and, therefore, make it bioavailable and toxic to plants.

However, low-ENP limestone presented a more complex mineral assemblage and a varied chemical composition. Lime with high ENP present a mineralogical composition based mainly on calcite and dolomite (i.e., predominately composed of Ca and Mg, respectively). The limestone quality is associated with its mineralogical assemblage, chemical composition, and granulometric profile. Thus, the ideal lime products are those composed of small mineral particles or nanoparticles (<10 µm) that are predominantly composed of calcite, dolomite, periclase, and low contents of accessory minerals in the assemblage. The small limestone particles are able to (i) migrate easily in the macropores, mainly in NT system [6], and (ii) neutralize H⁺ in soil depth [1,3,13].

Nevertheless, the Mg content seems to affect the GP of the peak positions. As laser diffraction provides a detailed GP ranging from nanometric to micrometric scale, and it is sensitive to pre-treatments, material reactivity can be estimated [5,15,21–23]. In this sense, limestone containing dolomite and calcite does not have the same GP. In addition, higher-ENP lime contains finer particles than low-ENP lime. Moreover, the presence of a larger volume of particles smaller than 10 µm is extremely important for rapid reactivity through the proton diffusion mechanism from the solution to the surface of the particles [24], ensuring total neutralization of the surrounding Al³⁺ because the dissolution rate is linear up to pH 5.0–5.5.

The dissolution of larger particles is hampered by the fact that the volume of the Diffusion Boundary Layer—DBL accessible to the proton is smaller. The center of the limestone particle is not accessible to the proton that diffuses from the soil solution, and consequently, the DBL is then low in proton activity and saturated with Ca and Mg, and the particle can even remain in the soil unchanged for a long time. The dissolution process is therefore kinetically dependent, sensitive to the pH values, pCO₂, Ca, and Mg activity of the solution [24–27]. Furthermore, in the kinetic mechanism (pH > 5.5 or coarser particles), in addition to Ca and Mg, the presence of phosphate ions, sulfate, silicates, and organic acids in the surrounding soil solution are inhibitors of dissolution, especially of dolomite or calcites altered by the presence of low Mg concentrations [26,28].

The dissolution rate of pure Mg carbonates (magnesite) is also linear up to pH 5 due to the proton adsorption mechanism on the particle surface. However, there is a requirement for protonation of four Mg-CO₃⁻ functional groups compared to only two of calcite (Ca-CO₃⁻). Additionally, the greater dependence of proton activity in solution on

dissolving magnesite is due to the shorter distance of the Mg-O bond (2.10 Å) compared to 2.36 Å of that of Ca-O [27].

Which lime is desirable for liming acid soils? At the beginning of conservationist systems (no-tillage, in particular) and of perennial/semi-perennial crops (tree and forage crops) from natural biomes or cultivated areas with intense soil disturbance, limestone should be homogenized with the maximum soil volume possible or required by the crops [1,11]; generally, this is in the 0–20 cm layer for annual crops and 0–40 cm layer for tree crops. The natural potential acidity in the soil profile can only be adequately corrected by the incorporation of lime. In this regard, all limestone particles are expected to be bathed by the acidic soil solution and, therefore, the particles are quickly dissolved and every soil mass reaches a predetermined pH value of pH 5.5 to 6.5, depending on the plant group involved [29]. The types of limestone, and even their grain size if it is less than 300 µm, are of little relevance.

However, controlling soil reacidification, which takes place from the surface, can and should be done by simply depositing lime on the soil surface [12]. This practice can be performed to prevent the resurgence of toxic Al³⁺ and/or to re-elevate the soil pH to the appropriate/desired level. Although the reactions in the dissolution of limestone particles and the consequent neutralization of active acidity, exchangeable Al³⁺, and potential acidity, will be concentrated in the uppermost soil layer (up to 5 cm), it is fundamental that extremely fine particles move down the soil profile, counterbalancing the acidifying power of the root system. Limestone containing large proportions of particles smaller than 10 µm or with total particles smaller than 25 µm, such as those in samples 11 and 14 (high and low MgO content, respectively), should be preferred for this purpose. In this sense, particle migration can occur preferentially for a certain particle size through the soil profile [5].

This is important in a no-till system where lime is applied on the topsoil when the moisture condition for the dissolution process [30] indicates that the finest size (<0.25 mm) will result in high Ca and Mg content in dry matter and, consequently, the largest crop yield. This interpretation is according to the dynamic dissolution of rock powder when applied on the topsoil, where the granulometric profile is a preponderant factor [31,32].

Liming products must have a large number of neutralizing agents in its composition. This can be found when lime produces a good milling process and a high reactive capacity (RE). These characteristics are assured by the mining and industry process and laws. Thus, chemically, all lime can be adequately used by varying its dose to compensate for reactive and granulometric characteristics [4].

In addition, limestone containing dolomite should not be used as a criterium for the capability of lime to neutralize H⁺ in acid soils. However, after lime availability for buying, soil Ca and Mg requirements may be used as discriminatory criteria for choosing the lime type (dolomitic or calcitic).

Finally, liming products containing a wide range of minerals in its composition presents less EPN compared to products predominantly composed of calcic and dolomite minerals. This suggests a smaller variety of high-quality limestone to correct acidity in agricultural soils. However, a multi-elementary liming products containing Ca, Mg, and K can be interesting for wide liming purposes, despite their lower neutralizing power and reactivity. As lime is applied over the topsoil in no-till systems, limestone powder with low size-particle distribution and high reactivity is desirable [33]. These characteristics were found predominantly in calcitic/dolomitic limestone powders. The implications of our findings indicate that the industrial milling process should be revisited, because reactivity depends on the granulometric profile as well. Future studies may be carried out on the reactivity rate under different soil conditions, such as water soil contents, in order to estimate the mineral dissolution rate [34].

5. Conclusions

The present study provides support for an appropriate selection of limestone materials for liming purposes. We investigated in detail 52 liming products samples with regard to their chemical and mineral composition and associated grain-size distribution to understand limestone reactivity for liming purposes. Our results showed that low-ENP limestone is composed of a wide range of mineral compositions and granulometric profiles. However, high-ENP limestone has the finest range of size particles without Mg, while in limestone containing Mg, the granulometric profile is wider. Liming products containing dolomite are sensitive to HCl treatment, suggesting high reactivity and easy mineral dissolution as compared to other liming products.

Finally, liming products may be discriminated based on their chemical contents (Mg:Ca proportion), mineral composition, and granulometric profile. The combination of these liming product characteristics results in a theoretical reactivity (ENP) in the environment. Thus, our work contributes to a better understanding of limestone quality and serves to improve liming practices in acidic soils, mainly in undisturbed systems, such as no-till.

Author Contributions: Conceptualization: E.C.B. and J.E.F.; methodology: D.F.M. and A.G.; validation: E.C.B., D.R.d.S., T.T. and D.F.M.; formal analysis: A.G.; investigation: A.G.; resources: E.C.B. and J.E.F.; data curation: A.G.; writing—original draft preparation: A.G. and E.C.B.; writing—review and editing: E.C.B., T.T., D.F.M. and D.R.d.S.; visualization: D.R.d.S.; supervision: E.C.B.; project administration: E.C.B.; funding acquisition: J.E.F. and E.C.B. All authors have read and agreed to the published version of the manuscript.

Funding: The authors thank the National Council for Scientific and Technological Development (CNPq, Brazil) for fellowships awarded to A. Garibotti (BIC/CNPq), E.C. Bortoluzzi (304676/2019-5), D.S. Rheinheimer (309515/2015-7).

Institutional Review Board Statement: Not applicable.

Informed Consent Statement: Not applicable.

Data Availability Statement: Not applicable.

Acknowledgments: CCGL/RTC and FECOAGRO/RS by the support in offering the lime samples for this study.

Conflicts of Interest: The authors declare no conflict of interest.

References

1. Rheinheimer, D.S.; Tiecher, T.; Gonzatto, R.; Santanna, M.A.; Brunetto, G.; da Silva, L.S. Long-term effect of surface and incorporated liming in the conversion of natural grassland to no-till system for grain production in a highly acidic sandy-loam Ultisol from South Brazilian Campos. *Soil Tillage Res.* **2018**, *180*, 222–231. <https://doi.org/10.1016/j.still.2018.03.014>.
2. Nolla, A.; Alves, E.O.; Silva, T.; Bordin, A.V. Correção da acidez e disponibilização de fósforo e potássio em Latossolo vermelho distrófico típico submetido à calagem incorporada e superficial. *Braz. J. Anim. Environ. Res.* **2020**, *3*, 2478–2487. <https://doi.org/10.34188/bjaerv3n3-156>.
3. Kaminski, J.; Rheinheimer, D.S.; Gatiboni, L.C.; Brunetto, G.; Silva, L.S. Eficiência da calagem superficial e incorporada precedendo o sistema plantio direto em um Argissolo sob pastagem natural. *Rev. Bras. Cienc. Solo* **2005**, *29*, 573–580.
4. Haby, V.A.; Leonard, A.T. Limestone quality and effectiveness for neutralizing soil acidity. *Commun. Soil Sci. Plant Anal.* **2002**, *33*, 2935–2948. <https://doi.org/10.1081/CSS-120014492>.
5. Bortoluzzi, E.C.; Poleto, C.; Baginski, A.J.; da Silva, V.R. Aggregation of subtropical soil under liming: A study using laser diffraction. *Rev. Bras. Cienc. Solo* **2010**, *34*, 725–734. <https://doi.org/10.1590/S0100-06832010000300014>.
6. Silva, S.R.; dos Santos, H.P.; Lollato, R.P.; Santi, A.; Fontaneli, R.S. Soybean Yield and Soil Physical Properties as Affected by Long-Term Tillage Systems and Liming in Southern Brazil. *Int. J. Plant Prod.* **2022**, *in press*. <https://doi.org/10.1007/s42106-022-00217-0>.
7. Olego, M.Á.; Quiroga, M.J.; López, R.; Garzón-Jimeno, E. The Importance of Liming with an Appropriate Liming Material: Long-Term Experience with a Typic Palexerult. *Plants* **2021**, *10*, 2605. <https://doi.org/10.3390/plants10122605>.
8. Embrapa. *Características de Corretivos Agrícolas*; Primavesi, A.C., Primavesi, O., Eds.; Embrapa Pecuária Sudeste: Brasília, Brazil, 2004; 28p.
9. Rodrighero, M.B.; Barth, G.; Caires, E.F. Aplicação superficial de calcário com diferentes teores de magnésio e granulometrias em sistema plantio direto. *Rev. Bras. Cienc. Solo* **2015**, *39*, 1723–1736. <https://doi.org/10.1590/01000683rbc20150036>.

10. Van Raij, B.; Sacchetto, M.T.D.; Kupper, A. Correlações entre o pH e o grau de saturação em bases nos solos com horizonte B textural e horizonte B latossólico. *Bragantia* **1968**, *27*, 493–500.
11. Bellinaso, R.J.; Tiecher, T.; Vargas, J.; Rheinheimer, D.S. Crop yields in no-tillage are severely limited by low availability of P and high acidity of the soil in depth. *Soil Res.* **2021**, *60*, 33–49. <https://doi.org/10.1071/SR21021>.
12. Rheinheimer, D.S.; Tiecher, T.; Gonzatto, R.; Zafar, M.; Brunetto, G. Residual effect of surface-applied lime on soil acidity properties in a long-term experiment under no-till in a Southern Brazilian sandy Ultisol. *Geoderma* **2018**, *313*, 7–16. <https://doi.org/10.1016/j.geoderma.2017.10.024>.
13. Rheinheimer, D.S.; Santos, E.J.S.; Kaminski, J.; Bortoluzzi, E.C.; Gatiboni, L.C. Changes in acid soil properties by superficial and incorporated liming on natural pasture. *Rev. Bras. Cienc. Solo* **2000**, *24*, 797–805. <https://doi.org/10.1590/S0100-0683200000400012>.
14. Embrapa. *Embrapa Manual de Métodos de Análise de Solo*, 3rd ed.; Empresa Brasileira de Pesquisa Agropecuária. Embrapa Solos; Embrapa: Brasília, Brazil, 2017; p. 577.
15. Bortoluzzi, E.C.; Parize, G.L.; Korchagin, J.; Silva, V.R.; Rheinheimer, D.S.; Kaminski, J. Soybean root growth and crop yield in response to liming at the beginning of a no-tillage system. *Rev. Bras. Cienc. Solo* **2014**, *38*, 262–271. <https://doi.org/10.1590/S0100-06832014000100026>.
16. Bortoluzzi, E.C.; Garbozza, L.; Guareschi, C.; Rheinheimer, D.S. Efeito da calagem na relação entre solo e água. *Rev. Bras. Cienc. Solo* **2008**, *32*, 2621–2628. <https://doi.org/10.1590/S0100-06832008000700003>.
17. Gomes, C.B. *Os Carbonatitos Cretácicos da Plataforma Brasileira e Suas Principais Características*; Instituto de Geociências da USP: São Paulo, Brazil, 2020; 253p. <https://doi.org/10.11606/9786586403008>.
18. Brasil Ministério da Agricultura, Pecuária e Abastecimento. *Manual de Métodos Analíticos Oficiais Para Fertilizantes e Corretivos*; Ministério da Agricultura, Pecuária e Abastecimento: Brasília, Brazil, 2017; p. 200.
19. Brindley, G.W.; Brown, G. *Crystal Structures of Clay Minerals and Their X-ray Identification*; Monograph No. 5; Mineralogical Society: London, UK, 1980; p. 495.
20. Webster, R. Statistics to support soil research and their presentation. *Eur. J. Soil Sci.* **2001**, *52*, 331–340. <https://doi.org/10.1046/j.1365-2389.2001.00383.x>.
21. Eshel, G.; Levy, G.J.; Mingelgrin, U.; Singer, M.J. Critical Evaluation of the Use of Laser Diffraction for Particle-Size Distribution Analysis. *Soil Sci. Soc. Am. J.* **2004**, *68*, 736. <https://doi.org/10.2136/sssaj2004.7360>.
22. Tonello, M.S.; Hebnar, T.S.; Sterner, R.W.; Brovold, S.; Tiecher, T.; Bortoluzzi, E.C.; Merten, G.H. Geochemistry and mineralogy of southwestern Lake Superior sediments with an emphasis on phosphorus lability. *J. Soils Sedim.* **2020**, *20*, 1060–1073. <https://doi.org/10.1007/s11368-019-02420-5>.
23. Ramos, C.G.; Oliveira, M.L.S.; Pena, M.F.P.; Cantillo, A.M.; Ayarza, L.P.L.; Korchagin, J.; Bortoluzzi, E.C. Nanoparticles generated during volcanic rock exploitation: An overview. *J. Environ. Chem. Eng.* **2021**, *9*, 106441. <https://doi.org/10.1016/j.jece.2021.106441>.
24. Morse, J.W.; Arvidson, R.S. The dissolution kinetics of major sedimentary carbonate minerals. *Earth-Sci. Rev.* **2002**, *58*, 51–84. <https://doi.org/10.1016/S0012-825200083-6>.
25. Sjöberg, E.L.; Rickard, D. The influence of experimental design on the rate of calcite dissolution. *Geochim. Cosmochim. Acta* **1983**, *47*, 2281–2285. <https://doi.org/10.1016/0016-703790051-0>.
26. Grunwaldt, H.S.; Zimina, A.; Göttlicher, J.; Steininger, R.; Grunwaldt, J.D. Study of the relation between Mg content and dissolution kinetics of natural lime stone using μ XRF, μ XRD and μ XAS. *J. Phys. Conf. Ser.* **2016**, *712*, 012144. <https://doi.org/10.1088/1742-6596/712/1/012144>.
27. Pokrovsky, O.S.; Schott, J. Processes at the magnesium-bearing carbonates/solution interface. II. Kinetics and mechanism of magnesite dissolution. *Geochim. Cosmochim. Acta* **1999**, *63*, 881–897. <https://doi.org/10.1016/S0016-703700013-7>.
28. Chou, L.; Garrels, R.M.; Wollast, R. Comparative study of the kinetics and mechanisms of dissolution of carbonate minerals. *Chem. Geol.* **1989**, *78*, 269–282. <https://doi.org/10.1016/0009-254190063-6>.
29. CQFS-RS/SC Comissão de Química e Fertilidade do Solo. *Manual de Calagem e Adubação Para os Estados do Rio Grande do Sul e de Santa Catarina*; Sociedade Brasileira de Ciência do Solo, Núcleo Regional Sul: Porto Alegre, Brazil, 2016.
30. Viadé, A.; Fernández-Marcos, M.L.; Hernández-Nistal, J.; Alvarez, E. Effect of particle size of limestone on Ca, Mg and K contents in soil and in sward plants. *Sci. Agric.* **2011**, *68*, 200–208. <https://doi.org/10.1590/S0103-90162011000200010>.
31. Scott, B.J.; Conyers, M.K.; Fisher, R.; Lill, W. Particle size determines the efficiency of calcitic limestone in amending acidic soil. *Aust. J. Soil Res.* **1992**, *43*, 1175–1185.
32. Korchagin, J.; Caner, L.; Bortoluzzi, E.C. Variability of amethyst mining waste: A mineralogical and geochemical approach to evaluate the potential use in agriculture. *J. Clean. Prod.* **2019**, *210*, 749–758. <https://doi.org/10.1016/j.jclepro.2018.11.039>.
33. Caires, E.F.; Barth, G.; Garbuio, F.J.; Churka, S. Soil acidity, liming and soybean performance under no-till. *Sci. Agric.* **2008**, *65*, 532–540.
34. Julien, J.-L.; Tessier, D. Rôles du pH, de la CEC effective et des cations échangeables sur la stabilité structurale et l’affinité pour l’eau du sol. *Etude Gest. Sols* **2021**, *28*, 159–179.